ACS Energy LETTERS

http://pubs.acs.org/journal/aelccp

PERSPECTIVE

Distinction between Capacitive and Noncapacitive Hysteretic Currents in Operation and Degradation of Perovskite Solar Cells

Germà Garcia-Belmonte*,† and Juan Bisquert†,‡

†Institute of Advanced Materials (INAM), Universitat Jaume I, 12006 Castelló, Spain

‡Department of Chemistry, Faculty of Science, King Abdulaziz University, Jeddah, Saudi Arabia

ABSTRACT: **Perovskite solar cells suffer from significant performance distortions under working conditions, usually known by the generic label of hysteretic effects. A classification of the fluctuations associated with current−voltage curves, centered on capacitance analysis, including measurements in voltage sweep, is provided here. Scan rate constitutes an easy-to-implement probing technique able to differentiate between capacitive and noncapacitive contributions to the overall hysteretic response. Capacitive hysteresis shows a distinctive response with scan rate and mainly originates at TiO_2 interfaces contacting perovskite materials. It relies on the interfacial ability to accommodate both ionic and electronic charges in a highly reversible way. Noncapacitive hysteresis points to the occurrence of interfacial energetics modification or contact reactivity caused by perovskite ionic motion. It exhibits positive values for reverse scans, in opposition to what is observed for capacitive currents. Connections between irreversible noncapacitve currents and device degradation are highlighted. The interfaces between the perovskite absorber and extracting layers play a determining role in the overall mechanisms of operation of this type of solar cell.**

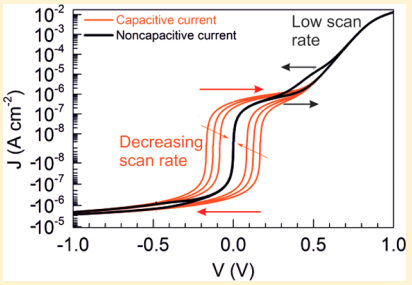

The development of lead halide perovskite solar cells[1−4] has produced a major upheaval in photovoltaic science and technology. Suddenly, for the first time major solar energy conversion efficiency has become available with solution-processed and low-cost methods. These light harvesting materials with the chemical formula ABX_3 are based on an organic cation, A, a metal cation, B, and a halide anion, X (A = methylammonium CH_3NH_3, MA, formamidinium $(NH_2)_2CH$; B = Pb, Sn; and X= Cl, Br, I). In particular, methylammonium lead iodide perovskite $MAPbI_3$ has been the object of extensive investigations, and it has become an archetypal example of these materials; however, other significant variants have been developed, including mixed perovskites that produce more stable devices.[5]

Even though excellent performance has been achieved and consolidated in these photovoltaic devices, it is also well-recognized that perovskite solar cells suffer from significant device performance fluctuations that constitute a major barrier for the further progress of energy conversion applications. The main type of fluctuation appears when measuring the current density−voltage (J−V) curve under illumination, and it is called current−voltage hysteresis, in which the shape of the curve depends on the way that the voltage sweep is realized.[6−8] In addition, a series of variations of performance related to illumination and applied voltage treatments have been widely reported.[9−11] In this Perspective we will summarize recent understanding of the performance fluctuations associated with current−voltage curves, based on a range of characterization techniques centered on capacitance, including the measurement of current during voltage scan in different cell configurations.

We start with the basic remark that the measurement of J−V curves is always a dynamic procedure in such a way that, apart from steady-state currents, transient currents may also contribute to the measured current level. This fact has led to recommendations on specific guidelines in measuring and reporting perovskite solar cell efficiencies.[12] The voltage variation, ΔV, applied to the solar cell produces a transient response before reaching the steady state. However, the time interval Δt between successive applied voltage steps might be shorter than the relaxation time. The ratio between voltage and time intervals allows one to establish the speed or scan rate $s = \Delta V/\Delta t$ of the measuring protocol. For constant scan rates of small voltage step with time, the voltage variation approximates a ramp, as occurs with the well-known cyclic voltammetry technique for the evaluation of electrochemical systems. In those cases in which charging mechanisms are present in the system, an additional transient current is expected to be

Received: July 23, 2016
Accepted: September 1, 2016

DOI: 10.1021/acsenergylett.6b00293
ACS Energy Lett. 2016, 1, 683−688

observed caused by the time variation of the accumulated charge Q[13]

$$J_{cap} = \frac{dQ}{dt} = C\frac{dV}{dt} = Cs \quad (1)$$

Equation 1 assumes the simplest response with a constant capacitance, C. Thereby capacitive currents, J_{cap}, appear as a consequence of a dynamic charging−discharging process depending on the scan rate magnitude and sign, as originally suggested in relation to the hysteresis response of perovskite solar cells.[9] Figure 1 illustrates some of the total current

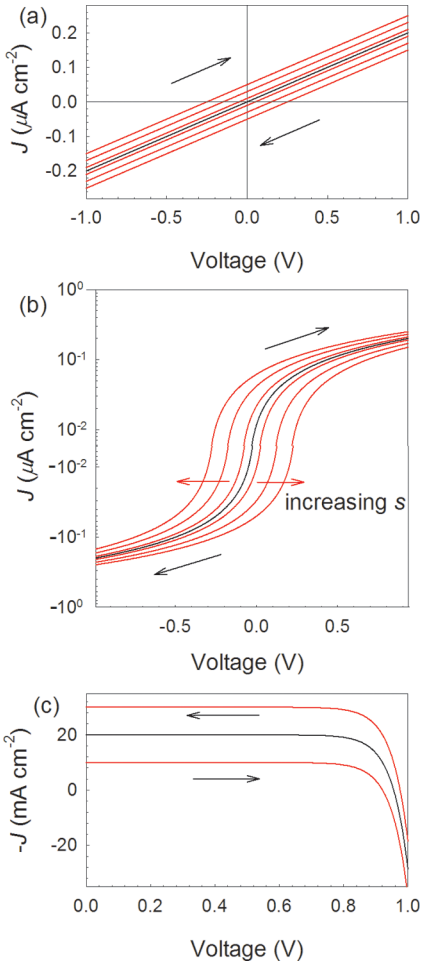

Figure 1. Simulated effect of scan rate increment on the $J-V$ curves including capacitive currents (red curves) in addition to an ohmic current (black curve) $J = J_{ohm} + J_{cap}$ in (a) linear and (b) log scaled current; (c) effect of capacitive currents on the generic $J-V$ curves under illumination, $J = J_{oper} + J_{cap}$. Black arrows indicate the sweep direction.

responses. When capacitive currents add up to a background ohmic dc current, one expects an opening up of the steady-state response featuring a broadening behavior that enlarges as s increases (Figure 1a). The crossing points at which current changes sign shift with the scan rate as observed in Figure 1b for log scaled currents. Interestingly, capacitive currents should vanish as the measuring speed approaches steady-state conditions as readily derived from eq 1. More generally, capacitive currents also appear in addition to operating currents under illumination, producing a broadening with respect to the steady-state response (Figure 1c). Capacitive currents are proposed to cause many of the observed experimental findings and reported phenomenology in hysteretic $J-V$ curves of perovskite solar cells, either in the dark or under illumination.[14,15] Electronic simulations that simply incorporate a capacitor in parallel to a generic diode and a current source accounting for the photocurrent qualitatively capture the main features of the $J-V$ curve hysteresis under illumination (Figure 2).[16]

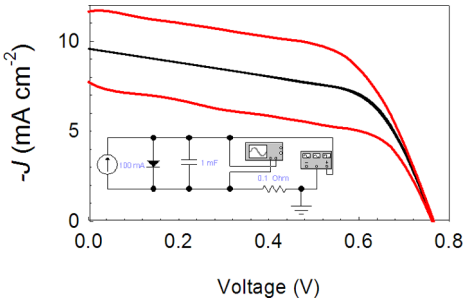

Figure 2. Example of $J-V$ curve under illumination using commercial simulation electronic software. The qualitative effect of the capacitor (red curves) is the broadening of the steady-state response (black curve) obtained without the capacitor. The inset shows the circuit used for the simulation.

> Capacitive currents are proposed to cause many of the observed experimental findings and reported phenomenology in hysteretic $J-V$ curves of perovskite solar cells.

The previously explained $J-V$ curve distortions caused by capacitive effect (capacitive hysteresis) have been regularly observed.[14,15] In Figure 3b one can identify how capacitive currents are visible in the dark operation of FTO/cTiO_2/mTiO_2/$MAPbI_3$/*spiro*-OMeTAD/Au structures.[17] Similar responses have been reported for planar solar cells comprising TiO_2.[14] On the other hand, experiments performed with inverted structures of the type ITO/PEDOT:PSS/$MAPbI_3$/$PC_{70}BM$/Ag (Figure 3c) clearly show the complete absence of capacitive current contributions. These contrasting responses are related to the low-frequency (∼1 Hz) capacitance features of the solar cells.[18] It is shown in Figure 4a that TiO_2-containing devices exhibit prominent capacitance values (∼50 $\mu F\,cm^{-2}$) in excess of geometrical capacitance. The effect is even bigger in the case of illumination, giving rise to capacitances as large as 1 $mF\,cm^{-2}$ as observed in Figure 4b.[18] In contrast, solar cells including organic and fullerene materials in contact layers show only small increments with respect to the geometrical capacitance values (Figure 4a).[17,19] These results indicate that "hysteresis free" devices significantly reduce capacitive currents by lowering capacitance mechanisms observed in the low-frequency part of the spectra. Conversely, the specific properties of the TiO_2/perovskite interface produce strong charge accumulation, both ionic and electronic, at this contact, giving rise to the capacitive hysteretic responses.

Besides observations of capacitive currents in the dark, the detailed exploration of stepwise transient currents has revealed that the elapsed time, Δt, between voltage steps, ΔV, readily determines the $J-V$ curve broadening around the steady-state

DOI: 10.1021/acsenergylett.6b00293
ACS Energy Lett. 2016, 1, 683−688

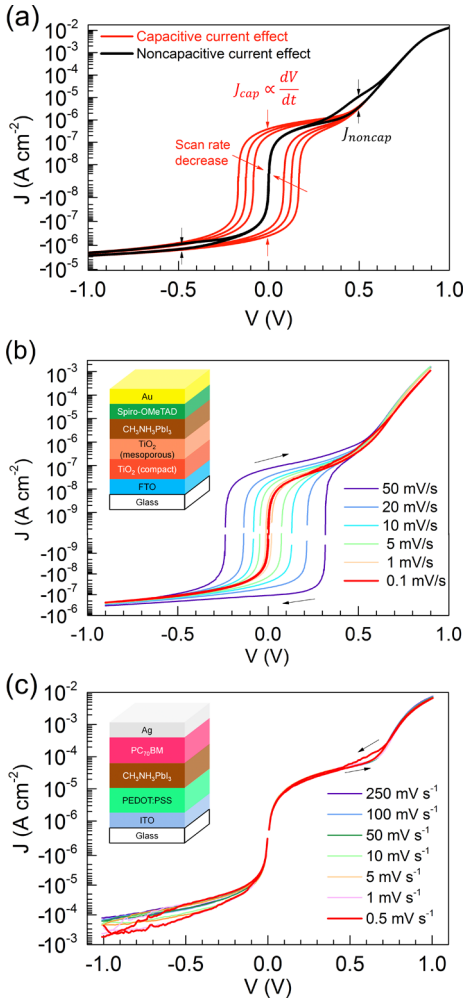

Figure 3. Dark *J*−*V* curves at room temperature in logarithm scaled current representation: (a) simulation illustrating different hysteretic effects as a function of the scan rate during the bias sweep in both senses; (b) cTiO$_2$/mTiO$_2$/MAPbI$_3$/*spiro*-OMeTAD and (c) PEDOT:PSS/MAPbI$_3$/PC$_{70}$BM PSCs at different scan rates with corresponding structures sketched in the insets. Reproduced from ref 17. Copyright 2016 American Chemical Society.

response.[15,20] As observed in Figure 5, for long Δt, current is able to reach steady-state levels, reducing the difference between forward to reverse voltage sweep response that is observed in the case of the shorter time steps.

A strong link is observed between the presence of TiO_2 layers contacting perovskite materials and the occurrence of capacitive hysteresis, manifested either in the dark or under illumination. In the dark, the interplay between ionic migrating species within the perovskite absorber and specific properties of the TiO_2/perovskite interface are the factor controlling the capacitive currents. Almora et al.[21] suggested that accumulation

A strong link is observed between the presence of TiO_2 layers contacting perovskite materials and the occurrence of capacitive hysteresis, manifested either in the dark or under illumination.

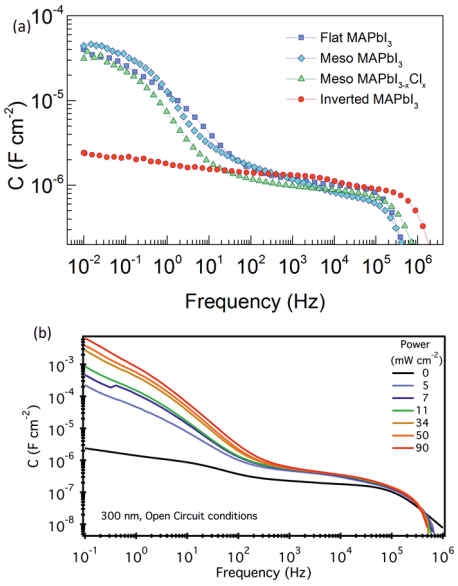

Figure 4. (a) Comparison of the capacitance spectra of a variety of perovskite solar cells with mesoporous or planar TiO_2 contacts (cTiO$_2$/mTiO$_2$/MAPbI$_{3-x}$Cl$_x$/*spiro*-OMeTAD, cTiO$_2$/mTiO$_2$/MAPbI$_3$/*spiro*-OMeTAD, and cTiO2/MAPbI$_3$/*spiro*-OMeTAD) and inverted (PEDOT:PSS/MAPbI$_3$/PC$_{70}$BM) structures measured in the dark at room temperature.; (b) effect of the illumination intensity on the low-frequency capacitance of CH(NH$_2$)$_2$PbI$_{3-x}$Cl$_x$-based planar solar cell. Reproduced from ref 31. Copyright 2016 American Chemical Society.

of ions at the interface in a double-layer structure is the main effect causing the large low-frequency capacitance. This is a highly reversible interfacial effect confined within short distances of the interface at the Debye length scale that is well-known in the contacts to ionic conductors.[22] The TiO_2/perovskite interface can easily accommodate charges in a highly reversible manner, giving rise to prominent capacitive currents and concomitant hysteretic distortions. This is corroborated by comparing the response of symmetrical devices: while TiO_2/perovskite/TiO_2 structures do exhibit pronounced capacitive currents, *spiro*-OMeTAD/perovskite/*spiro*-OMeTAD structures do not.[23] The substitution of TiO_2 by fullerene layers,[24] or just the deposition of fullerene molecules onto TiO_2,[25] suffices to significantly reduce the effect of capacitive hysteresis. It has been reported that the presence of organic layers at the contact interface cause a very different response to the contact TiO_2/perovskite, producing a large reduction of hysteresis.[26] The exact reason for this is not known, but reasonable explanations indicate that the organic contact provides a better surface match to the perovskite film compared with the metal oxide. The major increase of low-frequency capacitance can arise from two factors: TiO_2/perovskite mismatch may cause poor contact and voids at the interface that will provide enhanced polarization places. It has been also identified that the formation of weak Ti−I bounds at the contacts easily may accommodate ions in a highly reversible manner.[27] Instead, PCBM can absorb migration ions, compared with solid TiO_2 layer, which can smooth the double layer at the contact and reduce the low-frequency capacitance. In general, PCBM nanolayers modifying the TiO_2/perovskite interface produce a softening of the transition between the metal oxide and the perovskite that accommodates the charge and reduces the low-frequency capacitance by orders of magnitude, as in Figure 4.

DOI: 10.1021/acsenergylett.6b00293
ACS Energy Lett. 2016, 1, 683−688

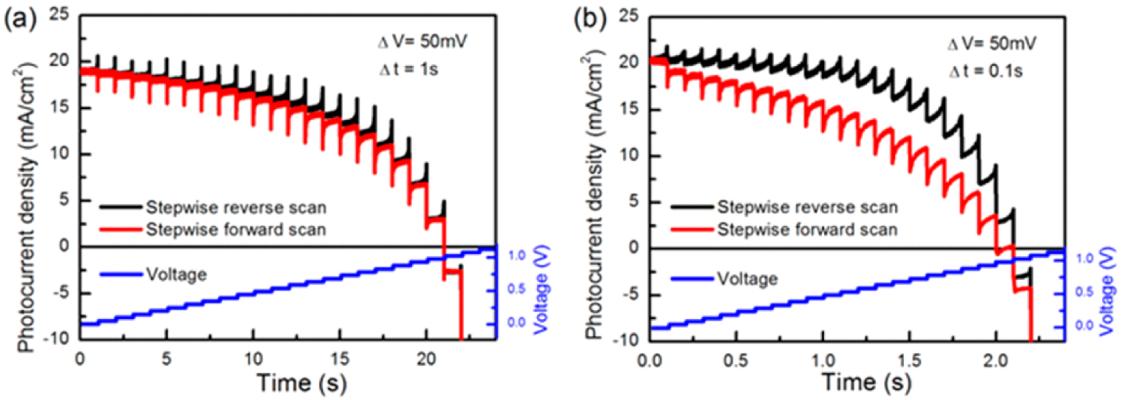

Figure 5. Time-dependent photocurrent response under reverse and forward stepwise scans with (a) 1 s step time and (b) 0.1 s step time of $cTiO_2$/$MAPbI_3$/*spiro*-OMeTAD solar cell architectures. Reproduced from ref 15. Copyright 2015 American Chemical Society.

Other dynamic modifications of the organic contact have been described, like the charge-transfer kinetics across the contact,[28] which can be severely modified by preconditioning.[29]

One of the effects of light irradiation of a perovskite solar cell is the dramatic enhancement of capacitive contributions.[18] The light capacitance has too large a value (>1 mF cm^{-2}) to be understood exclusively in terms of an ionic process. It is believed that perovskite traps and defects concentrate at the interfaces.[30] Electronic models based on the interfacial formation of accumulation zones have been proposed,[31] although additional evidence is needed to clarify the charge accumulation mechanism and the interplay between electronic and ionic dynamics. It should also be pointed out that a distinctive property of capacitive currents is their reduction as the measuring speed approaches steady-state conditions, as outlined in eq 1. Therefore, capacitive currents have only minor influence on the steady-state photovoltaic operation, having proved their reversibility.[23]

> Capacitive currents have only minor influence on the steady-state photovoltaic operation, having proved their reversibility.

Having described in detail the properties of capacitive contributions to hysteresis and their dependence on contact materials properties, we now point out that perovskite solar cells exhibit other *J*−*V* curve distortions that clearly lie outside of the range of capacitive charging phenomena. At slow enough scan rates additional features appear as those schematically drawn in Figure 3a (black curve).[17,23] At certain voltages, the *J*−*V* curves at forward and backward sweep separate from each other in such a way that a current contribution occurs in addition to the background level. This effect is clearly visible at ∼0.5−0.6 V for both regular and inverted architectures, as observed in Figure 3b,c. It is reported that this last kind of distortion current enlarges as the scan rate diminishes, thus signaling the noncapacitive nature of the underlying mechanism.[17] This is confirmed by the inverted response on sweep direction: noncapacitive currents exhibit positive values for reverse scans (Figure 3c), in opposition to what is observed for capacitive currents. Moreover, it shows a growing response after successive cycling for TiO_2/$MAPbI_3$/*spiro*-OMeTAD structures. Noncapacitive currents can be explained on the basis of a range of phenomena involving rearrangement of material properties, modification of interfaces,[32−34] or degradation effects. The observance of hysteresis in perovskite solar cells has been associated with changes of the interfacial electron-transfer barrier.[35] Several authors have indicated the connection between ionic migration and the modification of electronic barriers at the interface.[15,36] In contrast to this, other papers indicated the effect of ionic transport and band bending in the bulk perovskite material on *J*−*V* hysteresis.[37,38] A measurement of the *J*−*V* curve necessarily involves a major variation of band bending inside the device. Accordingly, a phenomenon of ion drift in the perovskite solar cell occurs that will modify both the interfaces[33,39] and the bulk drift field in the device.[38,40] There is a lack of experimentally proven models able to unambiguously predict the influence of ionic dynamics on device operation. It is thus unclear if ionic pile-up is a local effect affecting exclusively the outer interfaces or, on the contrary, if large extent space charge zones penetrate into the perovskite bulk. Reactivity between mobile ions of the perovskite and contacting *spiro*-OMeTAD has been also proposed to explain noncapacitive redox peaks as Faradaic currents in reactive electrodes.[23] Particularly prominent are noncapacitive currents in the case of inverted solar cells with organic and fullerene contacting materials.[17] In both cases noncapacitive currents should be understood as a manifestation of degradation processes taking place at the interface between perovskite and contacting materials.

> Noncapacitive currents can be explained on the basis of a range of phenomena involving rearrangement of material properties, modification of interfaces, or degradation effects.

The preceding account on the specific conditions yielding different hysteretic distortions in perovskite solar cell *J*−*V* curves allows us to establish a quantitative distinction between capacitive and noncapacitive currents. The variation of scan rate constitutes an easy-to-implement probing technique. The sketch of Figure 6 shows the different regions of influence of capacitive contributions depending on *s*. In the middle dynamic range, pure capacitive current is clearly revealed by proportional increase with scan rate. At high measuring speeds, the response *RC* time limits the charging of the capacitor so as to reduce the hysteresis, and consequently the magnitude of the capacitance

DOI: 10.1021/acsenergylett.6b00293
ACS Energy Lett. 2016, 1, 683−688

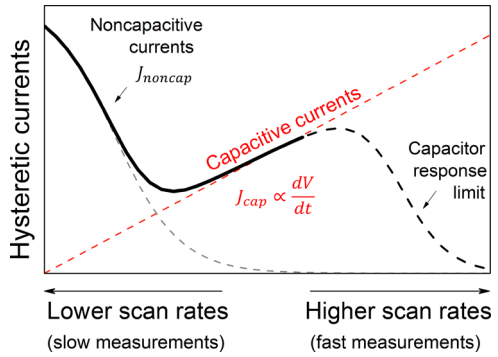

Figure 6. Schematic of the origin and repercussion of different hysteretic currents depending on the scan rate. Reproduced from ref 17. Copyright 2016 American Chemical Society.

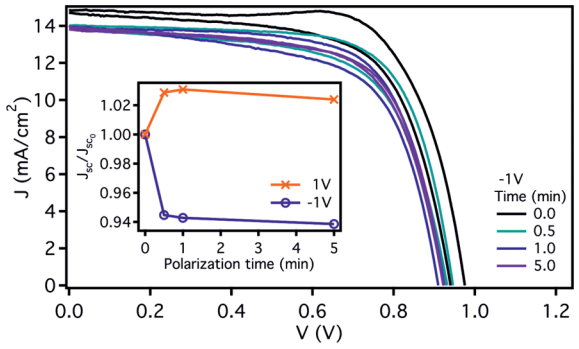

Figure 7. Effect of dark voltage pretreatment on $J-V$ response under illumination using a $cTiO_2/mTiO_2/MAPbI_3/spiro$-OMeTAD structure for different polarization time and negative polarization. The inset presents photocurrent variation for both positive and negative poling voltage.

is reduced, as observed in the high-frequency part of the capacitance spectra of Figure 4. This implies a maximum contribution of capacitive hysteresis at a certain scan rate, which should shift with temperature. At low enough scan rates a different phenomenology takes place: hysteretic currents enlarge as s is diminished, one of the fingerprints of noncapacitive currents. In addition, it exhibits an inverted response on sweep direction: positive hysteretic currents for backward scans. The dissimilar response points to the occurrence of different mechanisms. While capacitive currents are connected to the highly reversible charge accumulation ability of the TiO_2/perovskite interface, noncapacitive currents relate to injection barrier modification, transient charge accumulation phenomena that modify recombination and charge extraction rates, and irreversible chemical interactions between perovskite migrating ionic species and the contacting materials—*spiro*-OMeTAD, fullerenes, organic compounds, or diffusing metals of the contacts.

The previously outlined distinction between capacitive and noncapacitive contribution to the hysteretic currents does not yet complete the variety of effects found in experiments. For instance, a reduction in photocurrent has been reported for slow dynamic measurements attributed to the buildup of space charge close to the contacts.[41] In addition to the scan rate as a probing parameter, voltage pretreatment or poling is known to change dramatically the $J-V$ response of PSCs. Even the extreme case of reversing photocurrent by effect of poling has been reported.[42] In other structures, voltage pretreatment alters not only the hysteresis index (Figure 7) but also the resulting photocurrent measured at a constant scan rate. As observed in the inset of Figure 7, positive (+1 V) voltage polarization applied in the dark produces an increase in J_{sc} while the opposite effect occurs for negative (−1 V) pretreatment, in agreement with very recent reports.[43] This last observation points again to an alteration of the potential barriers at the interfaces that not only modifies the contact energetics but also changes the charge collection efficiency.

We can then conclude that interfaces between the perovskite absorber and the extracting layers, and the variety of local ionic or electronic mechanisms therein, play a determining role in the overall performance that this type of solar cell exhibits. Highly reversible ionic and (photogenerated carrier) electronic charge accumulation gives rise to electrode polarization (capacitive hysteresis), while noncapacitive currents are originated by rearrangement of material properties, modification of interfacial energetics, or degradation reactivity effects at the contacts. Further classification of experimental findings and modeling at the interface level is indeed necessary to progress in the identification of perovskite solar cell operating mechanisms.

AUTHOR INFORMATION

Corresponding Author

*E-mail: garciag@uji.es. Tel.: +34 964 387538.

Notes

The authors declare no competing financial interest.

ACKNOWLEDGMENTS

We thank Dr. I. Zarazua and O. Almora for their assistance in experiments. We acknowledge financial support by Ministerio de Economía y Competitividad (MINECO) of Spain under project (MAT2013-47192-C3-1-R) and Generalitat Valenciana (Prometeo/2014/020). SCIC at UJI are also acknowledged.

REFERENCES

(1) Kojima, A.; Teshima, K.; Shirai, Y.; Miyasaka, T. Organometal Halide Perovskites as Visible-Light Sensitizers for Photovoltaic Cells. *J. Am. Chem. Soc.* **2009**, *131*, 6050−6051.

(2) Im, J.-H.; Lee, C.-R.; Lee, J.-W.; Park, S.-W.; Park, N.-G. 6.5% Efficient Perovskite Quantum-Dot-Sensitized Solar Cell. *Nanoscale* **2011**, *3*, 4088−4093.

(3) Kim, H.-S.; Lee, C.-R.; Im, J.-H.; Lee, K.-B.; Moehl, T.; Marchioro, A.; Moon, S.-J.; Humphry-Baker, R.; Yum, J.-H.; Moser, J. E.; et al. Lead Iodide Perovskite Sensitized all-Solid-State Submicron Thin Film Mesoscopic Solar Cell with Efficiency Exceeding 9%. *Sci. Rep.* **2012**, *2*, 591.

(4) Lee, M. M.; Teuscher, J.; Miyasaka, T.; Murakami, T. N.; Snaith, H. J. Efficient Hybrid Solar Cells Based on Meso-Superstructured Organometal Halide Perovskites. *Science* **2012**, *338*, 643−647.

(5) Saliba, M.; Matsui, T.; Seo, J.-Y.; Domanski, K.; Correa-Baena, J.-P.; Nazeeruddin, M. K.; Zakeeruddin, S. M.; Tress, W.; Abate, A.; Hagfeldt, A.; et al. Cesium-Containing Triple Cation Perovskite Solar Cells: Improved Stability, Reproducibility and High Efficiency. *Energy Environ. Sci.* **2016**, *9*, 1989−1997.

(6) Snaith, H. J.; Abate, A.; Ball, J. M.; Eperon, G. E.; Leijtens, T.; Noel, N. K.; Stranks, S. D.; Wang, J. T.-W.; Wojciechowski, K.; Zhang, W. Anomalous Hysteresis in Perovskite Solar Cells. *J. Phys. Chem. Lett.* **2014**, *5*, 1511−1515.

(7) Unger, E. L.; Hoke, E. T.; Bailie, C. D.; Nguyen, W. H.; Bowring, A. R.; Heumuller, T.; Christoforo, M. G.; McGehee, M. D. Hysteresis and Transient Behavior in Current-Voltage Measurements of Hybrid-Perovskite Absorber Solar Cells. *Energy Environ. Sci.* **2014**, *7*, 3690−3698.

DOI: 10.1021/acsenergylett.6b00293
ACS Energy Lett. 2016, 1, 683−688

(8) Kim, H.-S.; Jang, I.-H.; Ahn, N.; Choi, M.; Guerrero, A.; Bisquert, J.; Park, N.-G. Control of I-V Hysteresis in $CH_3NH_3PbI_3$ Perovskite Solar Cell. *J. Phys. Chem. Lett.* **2015**, *6*, 4633−4639.
(9) Sanchez, R. S.; Gonzalez-Pedro, V.; Lee, J.-W.; Park, N.-G.; Kang, Y. S.; Mora-Sero, I.; Bisquert, J. Slow Dynamic Processes in Lead Halide Perovskite Solar Cells. Characteristic Times and Hysteresis. *J. Phys. Chem. Lett.* **2014**, *5*, 2357−2363.
(10) Gottesman, R.; Haltzi, E.; Gouda, L.; Tirosh, S.; Bouhadana, Y.; Zaban, A.; Mosconi, E.; De Angelis, F. Extremely Slow Photoconductivity Response of $CH_3NH_3PbI_3$ Perovskites Suggesting Structural Changes under Working Conditions. *J. Phys. Chem. Lett.* **2014**, *5*, 2662−2669.
(11) Gottesman, R.; Zaban, A. Perovskites for Photovoltaics in the Spotlight: Photoinduced Physical Changes and Their Implications. *Acc. Chem. Res.* **2016**, *49*, 320−329.
(12) Christians, J. A.; Manser, J. S.; Kamat, P. V. Best Practices in Perovskite Solar Cell Efficiency Measurements. Avoiding the Error of Making Bad Cells Look Good. *J. Phys. Chem. Lett.* **2015**, *6*, 852−857.
(13) Bisquert, J. *Nanostructured Energy Devices: Equilibrium Concepts and Kinetics*; CRC Press: Boca Raton, FL, 2014.
(14) Almora, O.; Zarazua, I.; Mas-Marza, E.; Mora-Sero, I.; Bisquert, J.; Garcia-Belmonte, G. Capacitive Dark Currents, Hysteresis, and Electrode Polarization in Lead Halide Perovskite Solar Cells. *J. Phys. Chem. Lett.* **2015**, *6*, 1645−1652.
(15) Chen, B.; Yang, M.; Zheng, X.; Wu, C.; Li, W.; Yan, Y.; Bisquert, J.; Garcia-Belmonte, G.; Zhu, K.; Priya, S. Impact of Capacitive Effect and Ion Migration on the Hysteretic Behavior of Perovskite Solar Cells. *J. Phys. Chem. Lett.* **2015**, *6*, 4693−4700.
(16) Cojocaru, L.; Uchida, S.; Jayaweera, P. V. V; Kaneko, S.; Nakazaki, J.; Kubo, T.; Segawa, H. Origin of the Hysteresis in I-V Curves for Planar Structure Perovskite Solar Cells Rationalized with a Surface Boundary-induced Capacitance Model. *Chem. Lett.* **2015**, *44*, 1750−1752.
(17) Almora, O.; Aranda, C.; Zarazua, I.; Guerrero, A.; Garcia-Belmonte, G. Noncapacitive Hysteresis in Perovskite Solar Cells at Room Temperature. *ACS Energy Lett.* **2016**, *1*, 209−215.
(18) Juarez-Perez, E. J.; Sanchez, R. S.; Badia, L.; Garcia-Belmonte, G.; Kang, Y. S.; Mora-Sero, I.; Bisquert, J. Photoinduced Giant Dielectric Constant in Lead Halide Perovskite Solar Cells. *J. Phys. Chem. Lett.* **2014**, *5*, 2390−2394.
(19) Kim, H.-S.; Jang, I.-H.; Ahn, N.; Choi, M.; Guerrero, A.; Bisquert, J.; Park, N.-G. Control of I−V Hysteresis in $CH_3NH_3PbI_3$ Perovskite Solar Cell. *J. Phys. Chem. Lett.* **2015**, *6*, 4633−4639.
(20) Kim, H.-S.; Park, N.-G. Parameters Affecting I−V Hysteresis of $CH_3NH_3PbI_3$ Perovskite Solar Cells: Effects of Perovskite Crystal Size and Mesoporous TiO_2 Layer. *J. Phys. Chem. Lett.* **2014**, *5*, 2927−2934.
(21) Almora, O.; Guerrero, A.; Garcia-Belmonte, G. Ionic Charging by Local Imbalance at Interfaces in Hybrid Lead Halide Perovskites. *Appl. Phys. Lett.* **2016**, *108*, 043903.
(22) Emmert, S.; Wolf, M.; Gulich, R.; Krohns, S.; Kastner, S.; Lunkenheimer, P.; Loidl, A. Electrode Polarization Effects in Broadband Dielectric Spectroscopy. *Eur. Phys. J. B* **2011**, *83*, 157−165.
(23) Carrillo, J.; Guerrero, A.; Rahimnejad, S.; Almora, O.; Zarazua, I.; Mas-Marza, E.; Bisquert, J.; Garcia-Belmonte, G. Ionic Reactivity at Contacts and Aging of Methylammonium Lead Triiodide Perovskite Solar Cells. *Adv. Energy Mater.* **2016**, *6*, 1502246.
(24) Shao, Y.; Xiao, Z.; Bi, C.; Yuan, Y.; Huang, J. Origin and Elimination of Photocurrent Hysteresis by Fullerene Passivation in $CH_3NH_3PbI_3$ Planar Heterojunction Solar Cells. *Nat. Commun.* **2014**, *5*, 5784.
(25) Wojciechowski, K.; Stranks, S. D.; Abate, A.; Sadoughi, G.; Sadhanala, A.; Kopidakis, N.; Rumbles, G.; Li, C.-Z.; Friend, R. H.; Jen, A. K.-Y.; et al. Heterojunction Modification for Highly Efficient Organic-Inorganic Perovskite Solar Cells. *ACS Nano* **2014**, *8*, 12701−12709.
(26) Wojciechowski, K.; Stranks, S. D.; Abate, A.; Sadoughi, G.; Sadhanala, A.; Kopidakis, N.; Rumbles, G.; Li, C.-Z.; Friend, R. H.; Jen, A. K. Y.; Snaith, H. J. Heterojunction Modification for Highly Efficient Organic−Inorganic Perovskite Solar Cells. *ACS Nano* **2014**, *8*, 12701−12709.
(27) Roiati, V.; Mosconi, E.; Listorti, A.; Colella, S.; Gigli, G.; De Angelis, F. Stark Effect in Perovskite/TiO2 Solar Cells: Evidence of Local Interfacial Order. *Nano Lett.* **2014**, *14*, 2168−2174.
(28) Tao, C.; Neutzner, S.; Colella, L.; Marras, S.; Srimath Kandada, A. R.; Gandini, M.; Bastiani, M. D.; Pace, G.; Manna, L.; Caironi, M.; Bertarelli, C.; et al. 17.6% Stabilized Efficiency in Low-Temperature Processed Planar Perovskite Solar Cells. *Energy Environ. Sci.* **2015**, *8*, 2365−2370.
(29) De Bastiani, M.; Dell'Erba, G.; Gandini, M.; D'Innocenzo, V.; Neutzner, S.; Kandada, A. R. S.; Grancini, G.; Binda, M.; Prato, M.; Ball, J. M.; et al. Ion Migration and the Role of Preconditioning Cycles in the Stabilization of the J−V Characteristics of Inverted Hybrid Perovskite Solar Cells. *Adv. Energy Mater.* **2016**, *6*, 1501453.
(30) Wu, X.; Trinh, M. T.; Niesner, D.; Zhu, H.; Norman, Z.; Owen, J. S.; Yaffe, O.; Kudisch, B. J.; Zhu, X.-Y. Trap States in Lead Iodide Perovskites. *J. Am. Chem. Soc.* **2015**, *137*, 2089−2096.
(31) Zarazua, I.; Bisquert, J.; Garcia-Belmonte, G. Light-Induced Space-Charge Accumulation Zone as Photovoltaic Mechanism in Perovskite Solar Cells. *J. Phys. Chem. Lett.* **2016**, *7*, 525−528.
(32) Yang, T.-Y.; Gregori, G.; Pellet, N.; Graetzel, M.; Maier, J. The Significance of Ion Conduction in a Hybrid Organic−Inorganic Lead-Iodide-Based Perovskite Photosensitizer. *Angew. Chem.* **2015**, *127*, 8016−8021.
(33) Azpiroz, J. M.; Mosconi, E.; Bisquert, J.; De Angelis, F. Defect Migration in Methylammonium Lead Iodide and its Role in Perovskite Solar Cell Operation. *Energy Environ. Sci.* **2015**, *8*, 2118−2127.
(34) van Reenen, S.; Kemerink, M.; Snaith, H. J. Modeling Anomalous Hysteresis in Perovskite Solar Cells. *J. Phys. Chem. Lett.* **2015**, *6*, 3808−3814.
(35) Xing, G.; Wu, B.; Chen, S.; Chua, J.; Yantara, N.; Mhaisalkar, S.; Mathews, N.; Sum, T. C. Interfacial Electron Transfer Barrier at Compact TiO_2/$CH_3NH_3PbI_3$ Heterojunction. *Small* **2015**, *11*, 3606−3613.
(36) Li, C.; Tscheuschner, S.; Paulus, F.; Hopkinson, P. E.; Kießling, J.; Köhler, A.; Vaynzof, Y.; Huettner, S. Iodine Migration and its Effect on Hysteresis in Perovskite Solar Cells. *Adv. Mater.* **2016**, *28*, 2446−2454.
(37) Meloni, S.; Moehl, T.; Tress, W.; Franckevičius, M.; Saliba, M.; Lee, Y. H.; Gao, P.; Nazeeruddin, M. K.; Zakeeruddin, S. M.; Rothlisberger, U.; et al. Ionic Polarization-Induced Current−Voltage Hysteresis in $CH_3NH_3PbX_3$ Perovskite Solar Cells. *Nat. Commun.* **2016**, *7*, 10334.
(38) Eames, C.; Frost, J. M.; Barnes, P. R. F.; O'Regan, B. C.; Walsh, A.; Islam, M. S. Ionic Transport in Hybrid Lead Iodide Perovskite Solar Cells. *Nat. Commun.* **2015**, *6*, 7497.
(39) van Reenen, S.; Kemerink, M.; Snaith, H. J. Modeling Anomalous Hysteresis in Perovskite Solar Cells. *J. Phys. Chem. Lett.* **2015**, *6*, 3808−3814.
(40) Richardson, G.; O'Kane, S. E. J.; Niemann, R. G.; Peltola, T. A.; Foster, J. M.; Cameron, P. J.; Walker, A. B. Can Slow-Moving Ions Explain Hysteresis in the Current-Voltage Curves of Perovskite Solar Cells? *Energy Environ. Sci.* **2016**, *9*, 1476−1485.
(41) Tress, W.; Marinova, N.; Moehl, T.; Zakeeruddin, S. M.; Nazeeruddin, M. K.; Gratzel, M. Understanding the Rate-Dependent J-V Hysteresis, Slow Time Component, and Aging in $CH_3NH_3PbI_3$ Perovskite Solar Cells: the Role of a Compensated Electric Field. *Energy Environ. Sci.* **2015**, *8*, 995−1004.
(42) Xiao, Z.; Yuan, Y.; Shao, Y.; Wang, Q.; Dong, Q.; Bi, C.; Sharma, P.; Gruverman, A.; Huang, J. Giant Switchable Photovoltaic Effect in Organometal Trihalide Perovskite Devices. *Nat. Mater.* **2015**, *14*, 193−198.
(43) Tress, W.; Correa-Baena, J.-P.; Saliba, M.; Abate, A.; Graetzel, M. Inverted Current−Voltage Hysteresis in Mixed Perovskite Solar Cells: Polarization, Energy Barriers, and Defect Recombination. *Adv. Energy Mater.* **2016**, 1600396.

DOI: 10.1021/acsenergylett.6b00293
ACS Energy Lett. 2016, 1, 683−688